EEG-fTCD Hybrid Brain-Computer Interface Using Template Matching and Wavelet Decomposition

Aya Khalaf*, Ervin Sejdic, Murat Akcakaya

Abstract

Objective. We aim at developing a hybrid brain-computer interface that utilizes electroencephalography (EEG) and functional transcranial Doppler (fTCD). In this hybrid BCI, EEG and fTCD are used simultaneously to measure electrical brain activity and cerebral blood velocity respectively in response to flickering mental rotation and word generation tasks. In this paper, we improve both the accuracy and information transfer rate (ITR) of this novel hybrid brain computer interface (BCI) we designed in our previous work. ***Approach.*** To achieve such aim, we focused on employing more advanced feature extraction and fusion techniques compared to the analysis techniques we applied previously. In particular, template matching was used to analyze EEG data whereas 5-level Wavelet decomposition was applied to fTCD data. EEG and fTCD feature vectors were combined using a Bayesian approach in a probabilistic manner different than the feature vector concatenation we performed before. Feature selection and classification were performed using Wilcoxon signed rank test and support vector machines respectively. ***Main results.*** Average accuracy and average ITR of 98.11% and 21.29 bits/min were achieved for WG versus MR classification while MR versus baseline yielded 86.27% average accuracy and 8.95 bit/min average ITR. In addition, average accuracy of 85.29% and average ITR of 8.34 bits/min were obtained for WG versus baseline. ***Significance.*** The proposed analysis techniques significantly improved the hybrid BCI performance. Specifically, for MR/WG versus baseline problems, we achieved twice of the ITRs obtained in our previous study. Moreover, the ITR of WG versus MR problem is 4-times the ITR we obtained before for the same problem. The current analysis methods boosted the performance of our EEG-fTCD BCI such that it outperformed the existing EEG-fNIRS BCIs in comparison.

***Index Terms*—Electroencephalogram, Functional Transcranial Doppler Ultrasound, Hybrid Brain-Computer Interfaces, Classification.**

1. Introduction

To enhance the performance of brain-computer interfaces (BCIs) in terms of accuracy and information transfer rate (ITR), recent studies suggested designing hybrid BCIs in which inference of user intent is based on data acquired from more than one source signal [1]. One of these signals has to be reflecting certain brain activity while the other signals do not have to be brain-related signals [2]. To acquire signals reflecting brain activity, sensing modalities such as electrocardiogram (EEG) [3], functional near infrared spectroscopy (fNIRS) [4], and functional

Electrical and Computer Engineering Department, University of Pittsburgh, PA, USA. Corresponding author's email: afk17@ pitt.edu).

magnetic resonance imaging (fMRI) [5] are used whereas modalities such as electromyogram (EMG) [6] and Electrooculography(EOG) [7] are usually employed in hybrid BCI design to acquire brain non-related signals [8].

In terms of source signals, hybrid BCIs can be categorized into 3 main classes including BCIs sensing brain and non-brain signals, BCIs sensing different brain signals using different modalities, and BCIs using single modality to sense different patterns of the same brain activity due to mental tasks with different nature [9]. EEG-fNIRS systems [10][11] are common examples of hybrid BCIs measuring different brain-related signals while EEG-EMG and EEG-EOG hybrid BCIs [6][7] represent the category that exploits brain and non-brain signals for hybrid BCI design. As for the third category, different EEG signals (steady state visually-evoked potential (SSVEP), motor imagery (MI), and P300) can be combined to design a hybrid BCI although being recorded using a single modality [12]. Tasks inducing such different signals can be designed using different stimulus modalities (visual, audio, and tactile) [9][13].

Among hybrid BCIs exploiting different brain sensing modalities, EEG-fNIRS systems are widely studied and considered for real-life BCI applications [14]. In contrast, EEG-fMRI systems have several disadvantages that limit their practical usage in BCI design since fMRI is an expensive non-portable equipment that requires controlled environment to perform efficiently [15]. For instance, EEG and fNIRS modalities were used to design asynchronous hybrid BCI in which the BCI user does not need any cue to initiate communication with the machine [16]. In this study, EEG and fNIRS data were recorded in response to motor execution tasks. Motor imagery (MI) tasks were employed for development of an EEG-fNIRS BCI in which occurrence of MI was detected using fNIRS modality while MI type was identified using EEG modality [17]. Moreover, many researchers exploited both motor execution and MI tasks to design hybrid EEG-fNIRS BCIs and it was found that the data from both modalities due to different tasks complement each other [18][19]. In another EEG-fNIRS study, 4 commands were decoded using mental arithmetic and motor execution tasks [20].

However, EEG-fNIRS hybrid BCIs require long task periods as well as baseline/resting period before/after performing each task since fNIRS has low temporal resolution. Recently, functional transcranial Doppler ultrasound (fTCD) has been studied as a faster alternative to fNIRS that can afford higher accuracies and ITRs when used solely in BCI design [21]. Moreover, in previous studies, we have shown that fTCD can be successfully employed in hybrid BCIs to provide improved performance when combined with EEG [22][23]. In particular, two visual presentation schemes were designed for the hybrid EEG-fTCD system with the aim of finding the most efficient visual presentation in terms of obtained accuracies and ITRs. In the first visual presentation, EEG and fTCD data were recorded simultaneously during right and left arm MI tasks [22] while in the second visual presentation, EEG and fTCD were acquired simultaneously in response to flickering mental rotation (MR) and word generation (WG) tasks [23]. It was found that flickering MR/WG visual presentation can provide higher accuracies compared to accuracies achieved using MI

tasks. However, ITRs due to MI tasks were higher than those obtained using flickering MR/WG visual presentation.

In this paper, we aim at improving the accuracies and ITRs of the system employing flickering MR/WG visual presentation. To achieve such aim, 3 binary selection problems were evaluated including MR versus baseline, WG versus baseline, and WG versus MR. Template matching was used to classify EEG data based on templates extracted from the training trials while fTCD data were analyzed using 5-level wavelet decomposition. Such wavelet analysis was shown before to be efficient for improving the performance of fTCD based BCIs employing MR and WG tasks [21]. Wilcoxon signed-rank test was used to statistically select significant features while classification tasks were performed using support vector machines (SVM) classifier. Moreover, instead of concatenating EEG and fTCD feature vectors for SVM classification, we developed a Bayesian framework to combine EEG and fTCD feature vectors under 3 different assumptions.

2. Materials and Methods

This section includes a detailed description of our experimental design, feature extraction, and feature selection methods as well as feature fusion and decision-making algorithms.

2.1. Experimental Design

A g.tec EEG system was used for EEG data collection using 16 electrodes placed over frontal, central, and parietal lobes at locations Fp1, Fp2, F3, F4, Fz, Fc1, Fc2, Cz, P1, P2, C1, C2, Cp3, Cp4, P5, and P6. Left mastoid was used as the reference for all participants. EEG data were bandpass-filtered using the g. USBamp bio-signal amplifier with corner frequencies 2 and 62 Hz. EEG data were also filtered using 4th order notch filters with corner frequencies 58 and 62 Hz.

SONARA TCD system with two 2 MHz transducers was used to record fTCD data. To monitor blood flow in middle cerebral arties (MCAs) which are responsible of 80% of blood perfusion in brain, an fTCD depth of 50 mm was selected and used during all data collection sessions [24]. The fTCD transducers were placed on both right and left sides of the transtemporal window above the zygomatic arch [25][26].

To design an efficient hybrid EEG-fTCD system, the MR and WG mental tasks presented to the BCI user have to be successfully identified by both recording modalities. However, MR and WG tasks are well known to be distinguished only using fTCD. More specifically, MR and WG tasks are known to induce different blood perfusion in brain hemispheres and thus different fTCD signals. In order to get differentiated using EEG, the visual icons representing MR and WG mental tasks are textured with a checkerboard pattern as shown in Fig.1. In addition, each task flickers with different frequency to elicit SSVEPs according to the flickering frequency of the task of interest. Therefore, these tasks can be distinguished since they will generate distinct EEG responses.

As seen in Fig.1, visual icons representing flickering MR and WG tasks as well as the fixation cross resembling the baseline are shown simultaneously on the screen. To elicit distinct SSVEPs, MR

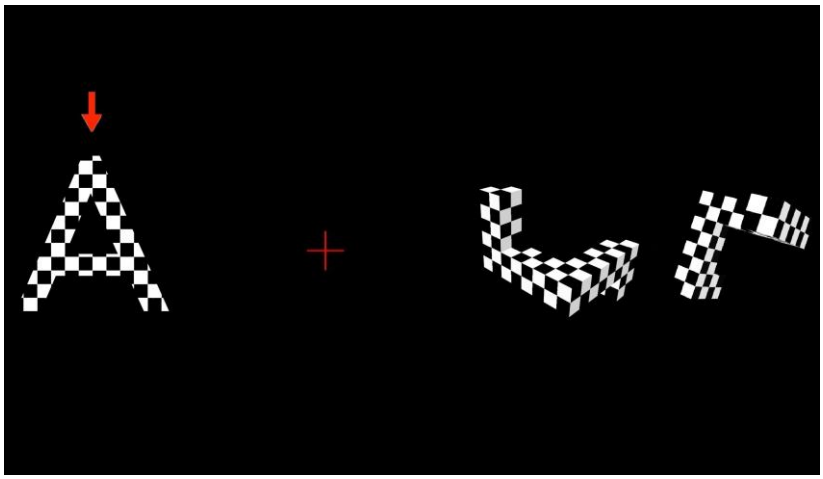

Fig. 1. Stimulus presentation of flickering MR/WG hybrid BCI system.

task flickers at 7Hz while WG task flickers at 17 Hz. At each trial, the red vertical arrow points randomly at one of the 3 icons for 10 s and the participant is asked to perform the mental task selected by the vertical arrow. For instance, to perform the WG task, the BCI user has to think about words starting with the letter shown on the screen. While the vertical arrow points to the MR task, the user has to mentally rotate one of the two 3D shapes shown on the screen and decide if the 2 shapes are identical or mirrored. Baseline data is collected when the vertical arrow points to the fixation cross. The user has to perform 150 randomized trials for 25 min.

University of Pittsburgh approved all research procedures under IRB number of PRO16080475. A total of 11 healthy participants signed informed consents and participated in the study including 3 females and 8 males with ages in the range from 25 to 32 years. Each of them attended one 25-min data collection session. None of these participants had a history of heart murmurs, migraines, strokes, or any brain related injuries.

2.2. Temporal Analysis

With the aim of finding the optimal task period, both EEG and fTCD data were analyzed and performance measures were evaluated across time. Calculated performance measures included accuracy and information transfer rate (ITR) [27] which is a measure the combines both accuracy and speed of the BCI. ITR is calculated as follows:

$$B = log_2(N) + Plog_2(P) + (1-P)log_2\left(\frac{1-P}{N-1}\right) \quad (1)$$

where P is the classification accuracy, N is the number of BCI classes, and B is the information transfer rate per trial.

For EEG data, an incremental window of 1-s initial width and 1-s increment size was used to infer the user intent across time while a 1-s width moving window with no overlap was used for the same purpose with the fTCD data. In particular, when generating the performance measures using EEG only, data of the EEG 1-s window were analyzed and performance measures were

calculated. Afterwards, the window size was increased by 1 s and performance measures were revaluated. Same process was carried out until the window width was equal to task period (10 s). Performance measures due to fTCD only were evaluated using a moving window of 1-s width instead of an incremental window. The choice of the moving window for fTCD analysis was based on a study we carried out before to enhance the performance of an fTCD-based BCI that employs MR and WG tasks [21].

To evaluate the performance of the hybrid combination, we developed a Bayesian framework that combines the evidences from fTCD and EEG modalities for joint user intent inference. At each time point (1, 2….,10 s), 1-D EEG and fTCD evidences corresponding to the EEG and fTCD feature vectors at that time point were generated. EEG and fTCD evidences corresponding to each time window were combined under 3 different assumptions including joint EEG-fTCD distributions, independent EEG and fTCD distributions as well as weighted independent EEG and fTCD distributions.

2.3. Feature Extraction

During each data collection session, 150 trials were presented to the BCI user. To extract features of each trial, both EEG and fTCD data corresponding to each 10-s trial were segmented. The data of each trial consisted of 16 EEG segments collected from the 16 EEG electrodes as well as 2 fTCD segments collected from the 2 fTCD transducers.

Cross correction coefficients generated using template matching represented EEG features while fTCD features were statistical features derived from the Wavelet decomposition of fTCD data corresponding to each trial. Features of all EEG/fTCD segments were concatenated to form EEG/fTCD feature vectors.

2.3.1. Template Matching

Instead of using canonical correlation analysis for analyzing EEG data in which artificial sinusoidal signals are used as reference signals to recognize frequency of the stimulus under test [28] [29], in this paper, templates generated from EEG training data were used as reference signals to identify the stimulus under test. In particular, each class has one template per EEG electrode and thus 16 templates per class were generated. The 16 templates corresponding to each class were obtained by averaging the training trials belonging to that class over each electrode location. Cross correlation coefficients between the 16 templates of each class and the corresponding 16 EEG segments of the trial under test were used as features, therefore, each EEG trial was represented by 32 features.

2.3.2. Wavelet Decomposition

To the best of our knowledge, the most efficient fTCD-based BCI in literature exploiting MR and WG mental tasks employed 5-level wavelet decomposition for feature extraction [21]. In this study, same analysis was applied to enhance the performance due to fTCD only and thus the

performance of the hybrid system. Specifically, 5-level Wavelet decomposition [30] was applied to the 2 fTCD data segments corresponding to each trial (one segment per fTCD channel). Daubechies 4 mother Wavelet was used to perform the decomposition. To reduce the dimensionality of the fTCD feature vector, 4 statistical features including mean, variance, skewness, and kurtosis [31] [32] were calculated for each of the 6 wavelet bands obtained from the decomposition leading to computation of 24 features per segment and 48 features per trial.

2.4. Feature Selection and Reduction

For both EEG and fTCD feature vectors, significant features were selected using Wilcoxon signed-rank test [33] at p-value of 0.05. However, for MR/WG versus baseline problems, Wilcoxon test with 0.05 significance level failed sometimes during some cross-validation folds to find significant features that distinguishes WG/MR task against baseline. Therefore, p-value of 0.1 was also used for task versus baseline problems and 2 sets of performance measures corresponding to p-values of 0.05 and 0.1 were generated. The best set of performance measures was reported in the results section (section 3) below. To evaluate the performance of single modality BCIs (EEG only and fTCD only BCIs), selected features from each modality were classified solely using support vector machine (SVM) classifier [34] and performance measures corresponding to each modality were generated.

EEG and fTCD feature vectors were combined to assess the performance of the hybrid system. Instead of concatenating the 2 feature vectors corresponding to each trial, SVM was used to reduce each feature vector of each trial into 1-D SVM score. In particular, 2 SVM classifiers were trained separately using selected EEG and fTCD feature vectors of the training trials. For each trail under test, the selected features from the 32-D EEG and 48-D fTCD feature vectors of that trial were reduced into 2 scalar SVM scores.

2.5. Feature Fusion and Decision Making

We designed a Bayesian framework to fuse EEG and fTCD evidences under 3 different assumptions including joint EEG-fTCD distributions ($A1$), independent EEG and fTCD distributions ($A2$) as well as weighted independent EEG and fTCD distributions ($A3$). EEG and fTCD evidences were partitioned randomly into training and testing sets using 10-fold cross validation scheme. Fig.2 illustrates $\mathrm{x_k}$ which is the latent dynamic state variable representing the unknown user intent at trial k that needs to be jointly inferred from a set of multimodal (EEG and fTCD) measurements $\mathrm{Y} = \{\mathrm{y}_1, \ldots \mathrm{y}_{N-10}\}$ where N is the number of trials presented to a BCI user. Note that the n^{th} measurement $\mathrm{y}_n = \{\mathrm{e}_n, \mathrm{f}_n\}$, includes both the EEG and fTCD evidences represented as e_n and f_n respectively. Inference of the unknown user intent $\mathrm{x_k}$ will be achieved through state estimation using the EEG and fTCD evidences jointly. Specifically, the following optimization problem will be solved.

$$\widehat{\mathrm{x_k}} = \arg\max_{\mathrm{x_k}} \mathrm{p}(\mathrm{x_k}|\mathrm{Y} = \mathrm{y}_k) \quad (2)$$

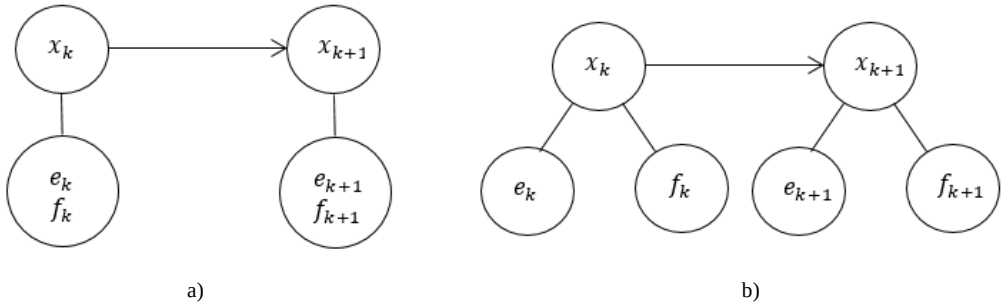

Fig. 2. Probabilistic graphical model illustrating the state and measurement relationships assuming EEG and fTCD evidences are jointly distributed (a) and independent (b).

In (2), $p(x_k|Y)$ is the posterior distribution of the state x_k conditioned on the observations Y. From Bayes rule, (2) is equivalent to:

$$\widehat{x_k} = \arg\max_{x_k} p(Y = y_k|x_k)\, p(x_k) \quad (3)$$

where $p(Y|x_k)$ is state conditional distribution of the measurements Y and $p(x_k)$ is the prior distribution defined over the values of state. Since the trials are randomized, we assume that $p(x_k)$ is uniformly distributed, then accordingly we rewrite (3) as:

$$\widehat{x_k} = \arg\max_{x_k} p(Y = y_k|x_k) \quad (4)$$

The distribution $p(Y|x_k)$ is computed from the training data. User intent at trial k is inferred by solving eqn. (4) at the measurement $Y = y_k$. In this study, the distribution $p(Y|x_k)$ was evaluated under 3 different assumptions.

2.5.1. Assumption 1: Joint Distribution

Since the k^{th} measurement is $y_k = \{e_k, f_k\}$, (4) can be written as:

$$\widehat{x_k} = \arg, \max_{x_k} p(e = e_k, f = f_k|x_k) \quad (5)$$

Where $p(e, f|x_k)$ is the state conditional joint distribution of *e* and *f*. This is represented graphically in Fig.2. a. To compute $p(e, f|x_k)$ for N-10 training trials, the joint distribution of the EEG and fTCD scores was assumed to follow a multivariate Gaussian distribution. Kernel density estimation with gaussian kernel was employed to compute the distributions $p(e, f|x_k), k = 1,2$. For measurements under test $y_k = \{e_k, f_k\}$, e_k and f_k are plugged in [5] and the user intent x_k that yields the maximum likelihood is selected.

2.5.2. Assumption 2: Independent Distributions

In order to compute $p(Y|x_k)$, we will assume that conditioned on the latent state, the EEG and fTCD evidences are independent from each other as seen in Fig.2.b, then accordingly also considering the uniform prior over the states, we rewrite (4) as:

$$\widehat{x_k} = \arg,\max_{x_k} p(e = e_k|x_k)p(f = f_k|x_k) \quad (6)$$

where $p(e|x_k)$ and $p(f|x_k)$ are the distributions of EEG and fTCD evidences conditioned on the state x_k respectively.

SVM EEG and fTCD scores of the N-10 training trials are used separately to compute 2 distributions [$(e|x_k)$ and $p(f|x_k)$] using kernel density estimation with gaussian kernel. For measurements under test $y_k = \{e_k, f_k\}$, e_k and f_k are plugged in (6) and the user intent x_k that yields the maximum likelihood is selected.

2.5.3. **Assumption 3: Weighted Independent Distributions**

Since the contribution of EEG and fTCD evidences towards making a correct decision might be unequal, we suggest weighting the distributions $p(e|x_k)$ and $p(f|x_k)$, and thus rewriting (5) as:

$$\widehat{x_k} = \arg,\max_{x_k} p(e = e_k|x_k)^{\alpha} p(f = f_k|x_k)^{1-\alpha} \quad (7)$$

Where α ranges from 0 to 1. $p(e|x_k)$ and $p(f|x_k)$ were computed as mentioned in section 5.2. These distributions were weighted with factors α and $1 - \alpha$ as seen in (7). This is equivalent to convex combination of the log likelihoods. Performance measures corresponding to α values ranging from 0 to 1 with a step of 0.05 were calculated and the best set of performance measures was reported in the results section (section 3) below. Due to computational complexity, α parameter was not optimized in this study. Instead, the best set of performance measures was reported. Herein, by inspecting performance measures obtained from $A3$ compared with those obtained from $A1$ and $A2$, $A3$ can be either excluded or considered in future studies with α parameter optimization so that the proposed system can be used in online settings.

3. Results

To evaluate the effectiveness of the hybrid system, maximum possible accuracy that can be obtained using EEG only and fTCD only was compared with the maximum accuracy achieved by the hybrid system under the 3 different assumptions ($A1$, $A2$, and $A3$) explained in section 2.5. These accuracies are reported in Tables 1,2, and 3 for MR vs baseline, WG versus baseline, and WG vs MR problems respectively. In addition, error bars of sensitivities and specificities corresponding to the accuracies listed in Tables 1,2, and 3 were plotted in Fig.3. Moreover, ITRs of $A1$, $A2$, $A3$, EEG only, and fTCD only were compared in Fig. 4. P-values showing the statistical significance of $A1$, $A2$, and $A3$ compared to EEG only and fTCD were calculated using Wilcoxon signed rank test and reported in Table 4.

As seen in Table 1, for MR versus baseline problem, $A1$, $A2$, and $A3$ achieved significantly higher average accuracies compared to EEG only and fTCD only. In particular, 79.45%, 83.24%, and 86.27% average accuracies were achieved by $A1$, $A2$, and $A3$ while EEG only and fTCD only obtained average accuracies of 75.28% and 68.66% respectively. As shown in Fig.3, error bars of the corresponding sensitivities and specificities show that $A2$ and $A3$ has the highest average

values and lowest standard deviation across participants especially compared to EEG only. Although $A1$, $A2$, and $A3$ outperformed EEG only and fTCD only in terms of average accuracy, $A1$ outperformed EEG for only 8 out of 11 participants while $A2$ and $A3$ outperformed EEG for 9 and 10 out of 11 participants respectively. Moreover, both $A2$ and $A3$ scored higher accuracies than fTCD only for all the participants while $A1$ outperformed fTCD only for 10 out of 11 participants. In line with these observations, p-values of Table 4 showed that $A1$ is not statistically significant compared to EEG only. Meanwhile, both $A2$ and $A3$ are statistically significant compared to EEG only. Compared to fTCD only, $A1$, $A2$, and $A3$ are statistically significant. In terms of ITRs, as seen in Fig.4.a, $A3$ outperformed $A1$, $A2$, EEG, and fTCD for most of the participants. On average, as shown in Fig.4. d., $A3$ achieved 8.95 bits/min while $A1$, $A2$, EEG, and fTCD yielded 7.55, 5.14, 3.49, and 2.46 bits/min respectively.

Tables 2 shows comparison of the performance measures obtained for WG versus baseline problem. $A1$, $A2$, and $A3$ obtained 78.26%, 82.85%, 85.29% average accuracy compared to %68.04, and 67.67% obtained by EEG only and fTCD only. As shown in Fig 3.b, the corresponding sensitivities and specificities have very similar values especially those of $A1$ and $A2$, therefore, the proposed classification model is balanced. In addition, $A2$ and $A3$ obtained higher accuracies than EEG only and fTCD only for all 11 participants. However, $A1$ achieved higher accuracies than EEG only and fTCD only for 9 and 10 participants respectively. These results are supported by the p-values of WG versus baseline problem listed in Table 4. Fig.4. b. shows that $A1$, $A2$, and $A3$ yielded higher ITRs for most of the participants compared to EEG only and fTCD. Unexpectedly, $A2$ obtained higher average ITR than $A3$ as shown in Fig.4. d. In particular, $A2$ obtained 8.89 bits/min while $A3$ obtained 8.34 bits/min. Meanwhile, $A1$, EEG only, and fTCD only got ITRs of 5.11, 1.98, and 1.37 bits/min respectively.

MR versus WG problem yielded the highest performance measures compared to MR/WG versus baseline problems as seen in Table 3. More specifically, $A1$, $A2$, and $A3$ obtained average accuracies of 97.84%, 97.40%, and 98.18% compared to 79.65% obtained by EEG only and 66.93% by fTCD only. Moreover, $A1$, $A2$, and $A3$ showed very low variance in sensitivities of MR and WG tasks across participants compared to EEG only and fTCD only as shown in Fig.3. c. Supported by the p-values in Table 4, for all participants, $A1$, $A2$, and $A3$ yielded higher accuracies than EEG only and fTCD only. In addition, $A1$, $A2$, and $A3$ achieved higher ITRs than EEG only and fTCD only for all participants as seen in Fig.4. c. In terms of average ITRs, as shown in Fig.4. d., EEG only obtained 3.62 bits/min while fTCD only obtained 2.84 bits/min. However, when combined together, $A1$, $A2$, and $A3$ yielded average ITRs of 20.99, 19.63, and 21.29 respectively.

TABLE 1

Maximum accuracy achieved for each subject using hybrid combinations (*A1*, *A2*, *A3*), EEG only, and fTCD only for MR vs baseline problem.

Sub_ID	EEG Accuracy	fTCD Accuracy	*A1*	*A2*	*A3*
1	68.75%	70.83%	80.21%	86.46%	91.67%
2	83.33%	60.42%	86.46%	89.58%	92.71%
3	78.13%	76.04%	83.33%	84.38%	87.50%
4	75.00%	65.63%	71.88%	76.04%	82.29%
5	73.96%	78.13%	75.00%	79.17%	81.25%
6	72.92%	64.58%	79.17%	80.21%	82.29%
7	78.13%	65.63%	82.29%	84.38%	85.42%
8	75.00%	65.63%	84.38%	89.58%	91.67%
9	58.33%	73.96%	84.38%	89.58%	91.67%
10	83.33%	68.75%	71.88%	76.04%	78.13%
11	81.25%	65.63%	75.00%	80.21%	84.38%
Mean	**75.28%**	**68.66%**	**79.45%**	**83.24%**	**86.27%**

TABLE 2

Maximum accuracy achieved for each subject using hybrid combinations (*A1*, *A2*, *A3*), EEG only, and fTCD only for WG vs baseline problem.

Sub_ID	EEG Accuracy	fTCD Accuracy	*A1*	*A2*	*A3*
1	79.38%	63.92%	81.44%	86.60%	88.66%
2	58.76%	62.89%	85.57%	90.72%	93.81%
3	75.26%	71.13%	85.57%	81.44%	84.54%
4	61.86%	61.86%	72.16%	78.35%	81.44%
5	70.10%	72.16%	70.10%	77.32%	79.38%
6	72.16%	74.23%	78.35%	78.35%	79.38%
7	63.92%	68.04%	78.35%	85.57%	88.66%
8	46.39%	72.16%	75.26%	81.44%	83.51%
9	72.16%	61.86%	82.47%	88.66%	91.75%
10	75.26%	64.95%	79.38%	85.57%	87.63%
11	73.20%	71.13%	72.16%	77.32%	79.38%
Mean	**%68.04**	**67.67%**	**78.26%**	**82.85%**	**85.29%**

TABLE 3

Maximum accuracy achieved for each subject using hybrid combinations (*A1*, *A2*, *A3*), EEG only, and fTCD only for MR vs WG problem.

Sub_ID	EEG Accuracy	fTCD Accuracy	*A1*	*A2*	*A3*
1	93.33%	62.86%	99.05%	99.05%	99.05%
2	81.90%	65.71%	100.0%	100.0%	100.0%
3	87.62%	68.57%	100.0%	100.0%	100.0%
4	75.24%	62.86%	100.0%	100.0%	100.0%
5	78.10%	64.76%	100.0%	96.19%	96.19%
6	72.38%	72.38%	99.05%	99.05%	99.05%
7	80.00%	70.48%	96.19%	95.24%	98.10%
8	72.38%	66.67%	83.81%	85.71%	88.57%
9	64.76%	69.52%	100.0%	100.0%	100.0%
10	90.48%	70.48%	100.0%	100.0%	100.0%
11	80.00%	61.90%	98.10%	96.19%	99.05%
Mean	**79.65%**	**66.93%**	**97.84%**	**97.40%**	**98.18%**

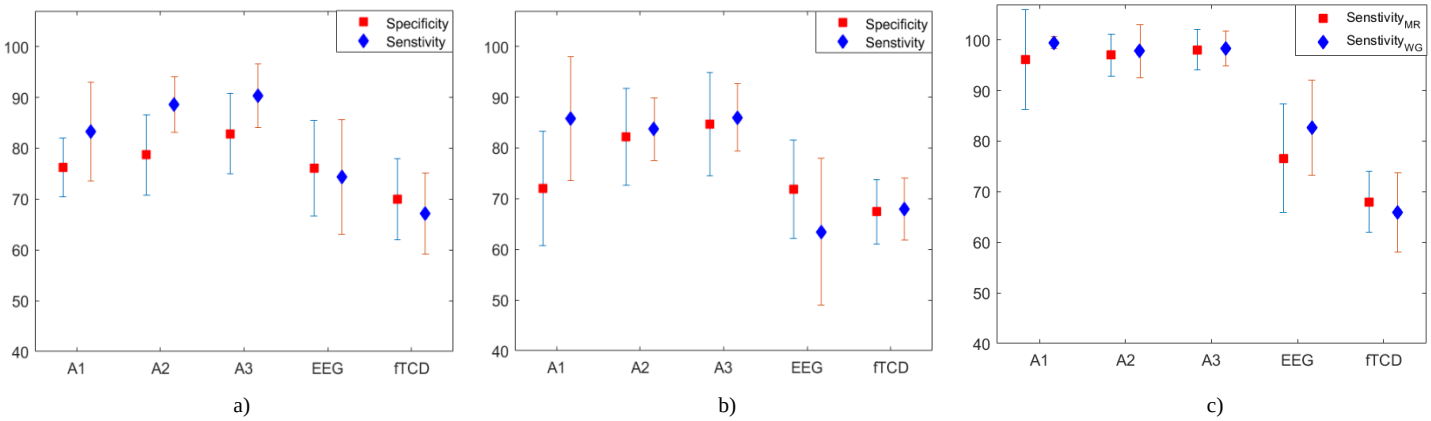

Fig. 3. Sensitivities and specificities (mean and standard deviation) calculated using *A1*, *A2*, *A3*, EEG only, and fTCD only for flickering MR vs baseline problem (a), flickering WG vs baseline problem (b), and flickering MR vs flickering WG (c).

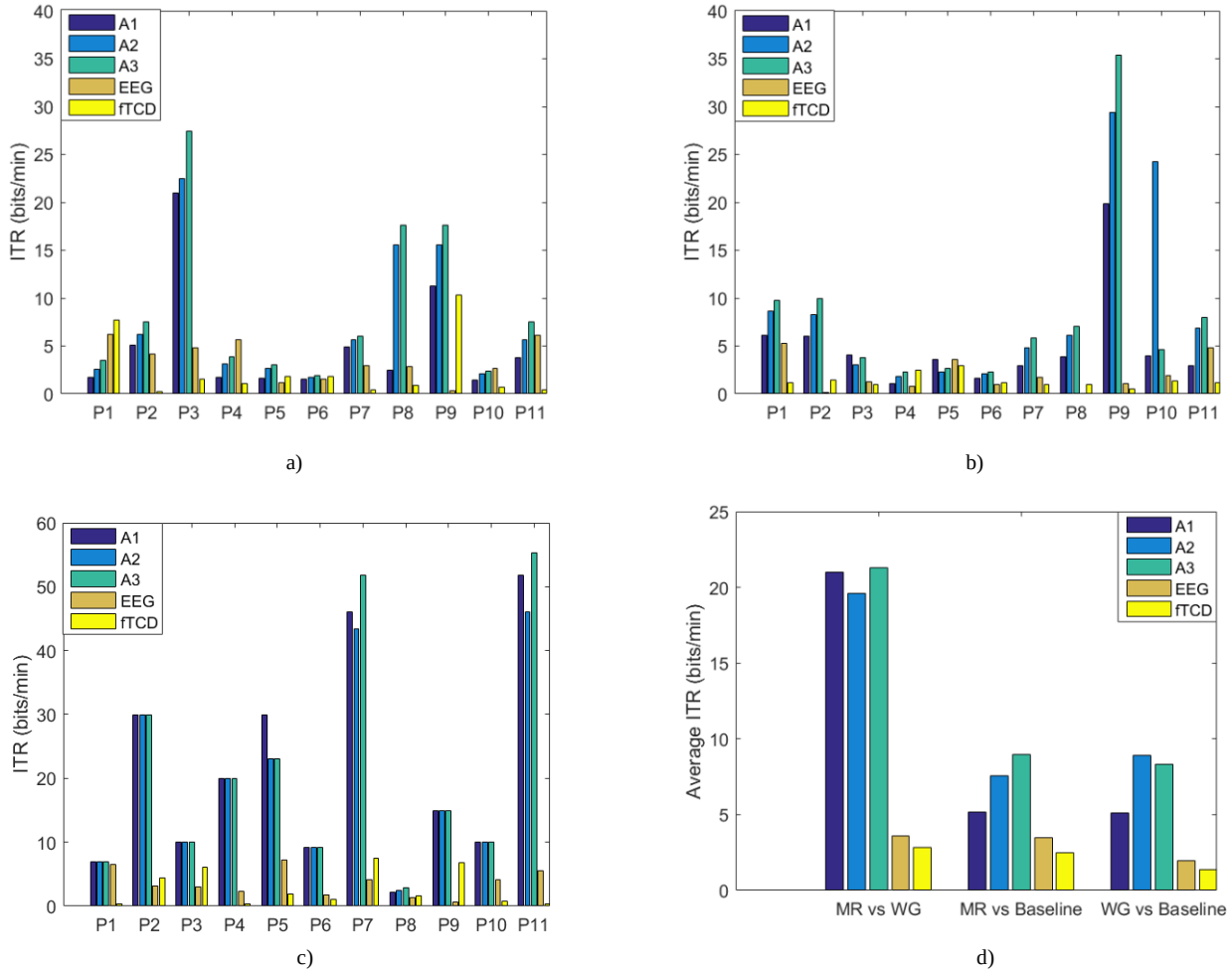

Fig. 4. Information transfer rates (ITRs) for each participant (P) calculated using EEG only, fTCD only, and the 3 hybrid combinations (*A1*, *A2*, and *A3*) for MR vs baseline problem (a), WG vs baseline problem (b), and MR vs WG problem (c). Average ITRs for the 3 problems are shown in subfigure (d).

TABLE 4
P-values showing \significance of *A1*, *A2*, and *A3* compared to EEG only and fTCD only for the 3 binary problems.

Comparison	MR vs Baseline	WG vs Baseline	MR vs WG
A1/EEG	0.1816	0.0039	0.0009
A1/fTCD	0.0029	0.0029	0.0009
A2/EEG	0.0293	0.0009	0.0009
A2/fTCD	0.0009	0.0009	0.0009
A3/EEG	0.0029	0.0009	0.0009
A3/fTCD	0.0009	0.0009	0.0009

4. Discussion

Based on the accuracies shown in Tables 1,2, and 3 as well as the average ITRs shown in Fig.3.d, it can be noticed that EEG and fTCD independence hypothesis ($A2$) yielded more efficient performance compared to the general hypothesis where EEG and fTCD are assumed to be Jointly distributed ($A1$). Moreover, although weighted independence hypothesis ($A3$) offers higher accuracies compared to those obtained under $A2$, the increase in accuracy is not that significant considering the increase in computational complexity due to α parameter optimization required when combining EEG and fTCD evidences under $A3$ in online settings. Moreover, despite the differences in accuracies, the ITRs due to $A2$ and $A3$ are very close in value to each other. Therefore, we believe that the system can perform efficiently under the independence assumption ($A2$).

It was shown that MR versus WG problem obtained significantly higher average accuracy and average ITR compared to MR/WG versus baseline problems. Specifically, accuracies of 86.27%,85.29%, and 98.11% were obtained by MR versus baseline, WG versus baseline, and MR versus WG respectively while the same binary problems yielded average ITRs of 8.95,8.34, and 21.29 bits/min respectively. One limitation of this study is that the BCI user gets distracted while focusing on the fixation cross during the baseline trials since such user experiences flickering effect coming from both visual icons representing MR and WG tasks during those baseline trials. However, the user is less distracted by this flickering effect while performing MR and WG tasks since they are separated by larger distance on the screen as shown in Fig.1. Such flickering effect is the reason behind the significant difference in both accuracy and ITR obtained for MR versus WG problem compared to accuracy and ITR achieved for MR/WG versus baseline problems. To reduce the distraction encountered by the user during baseline trials, a screen with larger dimensions can be used instead of the current 15.6” laptop screen. Another solution is to reduce the size of the visual icons representing the MR and WG tasks. Another limitation of the current study is the long data collection sessions (25 min) which leads to user’s fatigue and eye strain due to long exposure to flickering objects. Therefore, in the future version of this system, each session will be divided into 2 separate sessions.

Compared to the preliminary results we obtained before using flickering MR/WG visual presentation, in this paper, we improved the ITRs for the 3 binary problems at least 2 times

compared to the ITRs we obtained previously. In particular, previously we obtained 4.39, 3.92, and 5.60 bits/min average ITRs for MR versus baseline, WG versus baseline, and MR versus WG respectively while in this work, ITRs of 8.95,8.34, and 21.29 bits/min were obtained for the same binary problems respectively. In terms of accuracy, as shown in Table 5, the analysis we performed in the previous study yielded 89.11%, 80.88%, and 92.38% average accuracy for MR versus baseline, WG versus baseline, and MR versus WG respectively compared to 86.27%,85.29%, and 98.11% obtained with the current analysis. It can be noted that the MR versus baseline problem achieved lower accuracy with the current analysis. However, it obtained twice the ITR obtained in the previous study where the ITR is known to be a measure that combines both accuracy and speed of the BCI system. Moreover, as shown in Table 5, the flickering MR/WG visual presentation with the current analysis outperforms the motor imagery hybrid EEG- fTCD BCI we designed before.

In terms of accuracy, as seen in Table 5, the flickering MR/WG visual presentation with the current analysis outperforms the state of the art hybrid EEG-fNIRS BCIs [16][17][18][19][20] [22] [23][35][36][37] especially the MR versus WG binary selection problem. In terms of trial length, the proposed system has the shortest trial length of 10 *s* compared to the other systems in literature. Moreover, the proposed system does not require baseline or rest period before or after performing each task. Instead, the baseline cross in this study is selected randomly without any specified order during the visual presentation since it is considered as one of the tasks that reflects the case when no action is required to be performed. Even though the systems introduced in [16][20][35] achieved accuracies comparable to ours, such systems are slower than the proposed system. In particular, the system introduced by Putze *et al.* [35] requires task period of 12.5 *s* and rest period of 20 *s* while the system introduced by Khan *et al.* [20] needs 5 *s* rest period and 10 *s* task period. Moreover, baseline and task periods of 6 *s* are required for the system proposed by Buccino *et al.*[16]. In addition, 2 of these 3 studies exploited motor execution to design their BCIs [16][20] while the proposed system is intended to be used in the future by individuals with disabilities, therefore, it does not require any movement to execute any BCI command.

5. Conclusion

In this paper, to improve the performance measures of the hybrid EEG-fTCD BCI we designed before, we employed template matching for EEG analysis and Wavelet decomposition for fTCD analysis. In this hybrid BCI, EEG and fTCD data are recorded simultaneously while a visual presentation showing flickering MR and WG tasks is presented to the BCI user. To assess the hybrid system performance, 3 classification problems were solved including MR versus baseline, WG versus baseline, and MR versus WG. Average accuracies of 86.27%, 85.29%, and 98.11 were obtained for MR versus baseline, WG versus baseline, and MR versus WG respectively while same problems achieved average ITRs of 8.95, 8.34, and 21.29 bits/min respectively. These performance measures outperform the preliminary results we obtained before using flickering MR/WG visual presentation. Moreover, the system with the current analysis outperforms the

hybrid EEG-fNIRS BCIs in literature in terms of accuracy and trial length. Such results show that the proposed hybrid BCI with the current analysis techniques is a promising step towards making such hybrid systems efficient to be used in real-life BCI applications.

TABLE 5

Comparison between the proposed hybrid system and the state of the art hybrid BCIs.

Method	Activity	Modalities	Accuracy	Trial length (s)	
				Task	Baseline/rest
[18] Fazli et al., 2012	Motor Imagery	EEG+fNIRS	83.20%	15	6/0
[18] Fazli et al., 2012	Motor Execution	EEG+fNIRS	93.20%	15	6/0
[19] Blokland et al., 2014	Motor Imagery	EEG+fNIRS	79.00%	15	0/30±3
[19] Blokland et al., 2014	Motor Execution	EEG+fNIRS	87.00%	15	0/30±3
[20] Khan et al., 2014	Mental Arithmetic	EEG+fNIRS	83.60%	10	0/5
[20] Khan et al., 2014	Motor Execution	EEG+fNIRS	94.70%	10	0/5
[35] Putze et al., 2014	Visual/auditory stimuli	EEG+fNIRS	94.70%	12.5±2.5	0/20 ±5
[36] Yin et al., 2015	Motor Imagery	EEG+fNIRS	89.00%	10	0/21±1
[17] Koo et al. 2015	Motor Imagery	fTCD+NIRS	88.00%	15	0/60
[16] Buccino et al., 2016	Motor Execution	EEG+fNIRS	72.20%	6	6/0
[16] Buccino et al., 2016	Motor Execution	EEG+fNIRS	94.20%	6	6/0
[37] Shin et al., 2017	Mental Arithmetic	EEG+fNIRS	88.20%	10	0/16±1
[22] Khalaf et al.,2017(right/baseline)	Motor Imagery	EEG+fTCD	88.33%	10	NA
[22] Khalaf et al.,2017(left/baseline)	Motor Imagery	EEG+fTCD	89.48%	10	NA
[22] Khalaf et al.,2017(right/left)	Motor Imagery	EEG+fTCD	82.38%	10	NA
[23] Khalaf et al.,2018 (MR/baseline)	SSVEP+ MR/WG	EEG+fTCD	89.11%	10	NA
[23] Khalaf et al.,2018 (WG/baseline)	SSVEP+ MR/WG	EEG+fTCD	80.88%	10	NA
[23] Khalaf et al.,2018 (MR/WG)	SSVEP+ MR/WG	EEG+fTCD	92.38%	10	NA
Proposed method (MR/baseline)	SSVEP+ MR/WG	EEG+fTCD	**86.27%**	10	NA
Proposed method (WG/baseline)	SSVEP+ MR/WG	EEG+fTCD	**85.29%**	10	NA
Proposed method (MR/WG)	SSVEP+ MR/WG	EEG+fTCD	**98.11%**	10	NA

*NA: Not applicable

6. References

[1] G. R. Müller-Putz, C. Breitwieser, F. Cincotti, R. Leeb, M. Schreuder, F. Leotta, M. Tavella, L. Bianchi, A. Kreilinger, A. Ramsay, M. Rohm, M. Sagebaum, L. Tonin, C. Neuper, and J. del R. Millán, "Tools for brain-computer interaction: a general concept for a hybrid BCI," *Front. Neuroinform.*, vol. 5, p. 30, Nov. 2011.

[2] G. Pfurtscheller, B. Z. Allison, G. Bauernfeind, C. Brunner, T. Solis Escalante, R. Scherer, T. O. Zander, G. Mueller-Putz, C. Neuper, and N. Birbaumer, "The hybrid BCI," *Front. Neurosci.*, vol. 4, p. 3, Apr. 2010.

[3] F. Lotte, M. Congedo, A. Lécuyer, F. Lamarche, and B. Arnaldi, "A review of classification algorithms for EEG-based brain–computer interfaces," *J. Neural Eng.*, vol. 4, no. 2, pp. R1–R13, Jun. 2007.

[4] N. Naseer and K.-S. Hong, "fNIRS-based brain-computer interfaces: a review," *Front. Hum. Neurosci.*, vol. 9, p. 3, Jan. 2015.

[5] N. Weiskopf, K. Mathiak, S. W. Bock, F. Scharnowski, R. Veit, W. Grodd, R. Goebel, and N. Birbaumer, "Principles of a Brain-Computer Interface (BCI) Based on Real-Time Functional Magnetic Resonance Imaging (fMRI)," *IEEE Trans. Biomed. Eng.*, vol. 51, no. 6, pp. 966–970, Jun. 2004.

[6] T. D. Lalitharatne, K. Teramoto, Y. Hayashi, and K. Kiguchi, "Towards Hybrid EEG-EMG-Based Control Approaches to be Used in Bio-robotics Applications: Current Status, Challenges and Future Directions,"

Paladyn, J. Behav. Robot., vol. 4, no. 2, pp. 147–154, Jan. 2013.

[7] J. Ma, Y. Zhang, A. Cichocki, and F. Matsuno, "A Novel EOG/EEG Hybrid Human–Machine Interface Adopting Eye Movements and ERPs: Application to Robot Control," *IEEE Trans. Biomed. Eng.*, vol. 62, no. 3, pp. 876–889, Mar. 2015.

[8] K.-S. Hong and M. J. Khan, "Hybrid Brain–Computer Interface Techniques for Improved Classification Accuracy and Increased Number of Commands: A Review," *Front. Neurorobot.*, vol. 11, p. 35, Jul. 2017.

[9] I. Choi, I. Rhiu, Y. Lee, M. H. Yun, and C. S. Nam, "A systematic review of hybrid brain-computer interfaces: Taxonomy and usability perspectives.," *PLoS One*, vol. 12, no. 4, p. e0176674, 2017.

[10] K.-S. Hong, M. J. Khan, and M. J. Hong, "Feature Extraction and Classification Methods for Hybrid fNIRS-EEG Brain-Computer Interfaces.," *Front. Hum. Neurosci.*, vol. 12, p. 246, 2018.

[11] S. Ahn and S. C. Jun, "Multi-Modal Integration of EEG-fNIRS for Brain-Computer Interfaces – Current Limitations and Future Directions," *Front. Hum. Neurosci.*, vol. 11, p. 503, Oct. 2017.

[12] S. Amiri, R. Fazel-Rezai, and V. Asadpour, "A Review of Hybrid Brain-Computer Interface Systems," *Adv. Human-Computer Interact.*, vol. 2013, pp. 1–8, Feb. 2013.

[13] E. Yin, T. Zeyl, R. Saab, D. Hu, Z. Zhou, and T. Chau, "An Auditory-Tactile Visual Saccade-Independent P300 Brain–Computer Interface," *Int. J. Neural Syst.*, vol. 26, no. 01, p. 1650001, Feb. 2016.

[14] A. von Luhmann, H. Wabnitz, T. Sander, and K.-R. Muller, "M3BA: A Mobile, Modular, Multimodal Biosignal Acquisition Architecture for Miniaturized EEG-NIRS-Based Hybrid BCI and Monitoring," *IEEE Trans. Biomed. Eng.*, vol. 64, no. 6, pp. 1199–1210, Jun. 2017.

[15] B. Z. Allison, E. W. Wolpaw, and J. R. Wolpaw, "Brain-computer interface systems: progress and prospects.," *Expert Rev. Med. Devices*, vol. 4, no. 4, pp. 463–74, Jul. 2007.

[16] A. P. Buccino, H. O. Keles, and A. Omurtag, "Hybrid EEG-fNIRS Asynchronous Brain-Computer Interface for Multiple Motor Tasks," *PLoS One*, vol. 11, no. 1, p. e0146610, Jan. 2016.

[17] B. Koo, H.-G. Lee, Y. Nam, H. Kang, C. S. Koh, H.-C. Shin, and S. Choi, "A hybrid NIRS-EEG system for self-paced brain computer interface with online motor imagery," *J. Neurosci. Methods*, vol. 244, pp. 26–32, Apr. 2015.

[18] S. Fazli, J. Mehnert, J. Steinbrink, G. Curio, A. Villringer, K.-R. Müller, and B. Blankertz, "Enhanced performance by a hybrid NIRS–EEG brain computer interface," *Neuroimage*, vol. 59, no. 1, pp. 519–529, Jan. 2012.

[19] Y. Blokland, L. Spyrou, D. Thijssen, T. Eijsvogels, W. Colier, M. Floor-Westerdijk, R. Vlek, J. Bruhn, and J. Farquhar, "Combined EEG-fNIRS Decoding of Motor Attempt and Imagery for Brain Switch Control: An Offline Study in Patients With Tetraplegia," *IEEE Trans. Neural Syst. Rehabil. Eng.*, vol. 22, no. 2, pp. 222–229, Mar. 2014.

[20] M. J. Khan, M. J. Hong, and K.-S. Hong, "Decoding of four movement directions using hybrid NIRS-EEG brain-computer interface," *Front. Hum. Neurosci.*, vol. 8, p. 244, Apr. 2014.

[21] A. Khalaf, M. Sybeldon, E. Sejdic, and M. Akcakaya, "A brain-computer interface based on functional transcranial doppler ultrasound using wavelet transform and support vector machines," *J. Neurosci. Methods*, vol. 293, pp. 174–182, Jan. 2018.

[22] A. Khalaf, E. Sejdic, and M. Akcakaya, "A Novel Motor Imagery Hybrid Brain Computer Interface using EEG and Functional Transcranial Doppler Ultrasound," *J. Neurosci. Methods, Under Rev.*, 2018.

[23] A. Khalaf, E. Sejdic, and M. Akcakaya, "Towards optimal visual presentation design for hybrid EEG—fTCD

brain–computer interfaces," *J. Neural Eng.*, vol. 15, no. 5, p. 056019, Oct. 2018.

[24] L. H. Monsein, A. Y. Razumovsky, S. J. Ackerman, H. J. W. Nauta, and D. F. Hanley, "Validation of transcranial Doppler ultrasound with a stereotactic neurosurgical technique," *J. Neurosurg.*, vol. 82, no. 6, pp. 972–975, Jun. 1995.

[25] N. Stroobant and G. Vingerhoets, "Transcranial Doppler ultrasonography monitoring of cerebral hemodynamics during performance of cognitive tasks: a review.," *Neuropsychol. Rev.*, vol. 10, no. 4, pp. 213–31, Dec. 2000.

[26] A. V. Alexandrov, M. A. Sloan, L. K. S. Wong, C. Douville, A. Y. Razumovsky, W. J. Koroshetz, M. Kaps, and C. H. Tegeler, "Practice Standards for Transcranial Doppler Ultrasound: Part I-Test Performance," *J. Neuroimaging*, vol. 17, no. 1, pp. 11–18, Jan. 2007.

[27] B. Obermaier, C. Neuper, C. Guger, and G. Pfurtscheller, "Information transfer rate in a five-classes brain-computer interface," *IEEE Trans. Neural Syst. Rehabil. Eng.*, vol. 9, no. 3, pp. 283–288, 2001.

[28] B. Thompson, Thompson, and Bruce, "Canonical Correlation Analysis," in *Encyclopedia of Statistics in Behavioral Science*, Chichester, UK: John Wiley & Sons, Ltd, 2005.

[29] M. Nakanishi, Y. Wang, Y.-T. Wang, and T.-P. Jung, "A Comparison Study of Canonical Correlation Analysis Based Methods for Detecting Steady-State Visual Evoked Potentials," *PLoS One*, vol. 10, no. 10, p. e0140703, Oct. 2015.

[30] D. Valencia, "Discrete Wavelet Transform Filter Bank Implementation," 2010. [Online]. Available: https://www.dsprelated.com/showarticle/115.php.

[31] D. N. Joanes and C. A. Gill, "Comparing measures of sample skewness and kurtosis," *J. R. Stat. Soc. Ser. D (The Stat.*, vol. 47, no. 1, pp. 183–189, Mar. 1998.

[32] P. H. Westfall, "Kurtosis as Peakedness, 1905 - 2014. R.I.P.," *Am. Stat.*, vol. 68, no. 3, pp. 191–195, 2014.

[33] R. C. Blair and J. J. Higgins, "A Comparison of the Power of Wilcoxon's Rank-Sum Statistic to That of Student's t Statistic under Various Nonnormal Distributions," *J. Educ. Stat.*, vol. 5, no. 4, p. 309, 1980.

[34] C.-W. Chih-Wei Hsu and C.-J. Chih-Jen Lin, "A comparison of methods for multiclass support vector machines," *IEEE Trans. Neural Networks*, vol. 13, no. 2, pp. 415–425, Mar. 2002.

[35] F. Putze, S. Hesslinger, C.-Y. Tse, Y. Huang, C. Herff, C. Guan, and T. Schultz, "Hybrid fNIRS-EEG based classification of auditory and visual perception processes.," *Front. Neurosci.*, vol. 8, p. 373, 2014.

[36] X. Yin, B. Xu, C. Jiang, Y. Fu, Z. Wang, H. Li, and G. Shi, "A hybrid BCI based on EEG and fNIRS signals improves the performance of decoding motor imagery of both force and speed of hand clenching," *J. Neural Eng.*, vol. 12, no. 3, p. 036004, Jun. 2015.

[37] J. Shin, K.-R. Müller, C. H. Schmitz, D.-W. Kim, and H.-J. Hwang, "Evaluation of a Compact Hybrid Brain-Computer Interface System," *Biomed Res. Int.*, vol. 2017, pp. 1–11, Mar. 2017.